AE8150
Special Topics: Aerodynamics and Propulsion: Airfoils

Final Project Report
Transonic Airfoil Design

Student Name: Aman Gilani
Student Number: 500879895
Instructor: Jeffrey W. Yokota
Submission by: 3rd December 2024

Table of Contents

List of Figures

Introduction and objective

The objective of this design project was to design a transonic airfoil that will fly at a subsonic speed, have a region of supersonic flow over its upper surface, and have a normal shock that decelerates the flow from supersonic to subsonic. The primary goal was to design a transonic airfoil for a propeller, maintaining the lift calculated using compressible flow at tip velocities between Mach 0.63 and 0.75. Propellers often experience performance losses at higher Mach numbers due to compressibility effects from a normal shock [1]. This project explores methods to overcome this limitation by refining airfoil design.

Transonic regimes pose unique challenges due to the simultaneous presence of subsonic and supersonic flow regions. At higher Mach numbers, shocks develop on the upper surface, leading to drag rise and lift loss. In this project, the loss of lift due to the normal shock will be compensated by redesigning a new lower surface using concepts learnt in AE8150.

Incompressible Joukowski Airfoil

Starting with the design of an incompressible Joukowski Airfoil, the objective of designing a Joukowski Airfoil was to implement a low thickness to chord ratio along with slight camber. Through the comparison of empirical data of current airfoils in use from the Aeronautical Research Association (ARA) database, It was learnt that propeller airfoils are thin (about 7% thickness to chord ratio) and lave low chamber with sharp leading and trailing edges [1].

Using a circle centered at X_c = -0.1 and Y_c = 0.12 for the Joukowski transformation a Joukowski airfoil was designed using the following equations, where θ ranges between 0 and 2π. The implication of varying X_c and Y_c, were discussed in the midterm project.

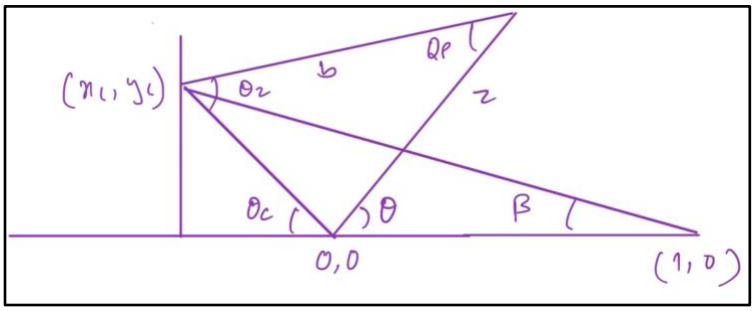

Figure 1: *Joukowski Transformation.*

$$\theta_c = \tan^{-1}\frac{y_c}{x_c}$$

$$\theta_b = \pi - \theta - \theta_c$$

$$b = \sqrt{(1 - x_c)^2 + (y_c)^2}$$

$$c = \sqrt{(x_c)^2 + (y_c)^2}$$

$$\theta_p = \sin^{-1}\left(\frac{c}{b} * \sin(\theta_b)\right)$$
$$\theta_z = \theta + \theta_c - \theta_p$$
$$\|Z\| = \frac{b * \sin(\theta_z)}{\sin(\theta_b)}$$
$$Z = \|Z\| * e^{\theta i}$$
$$\zeta = Z + \frac{1}{Z}$$

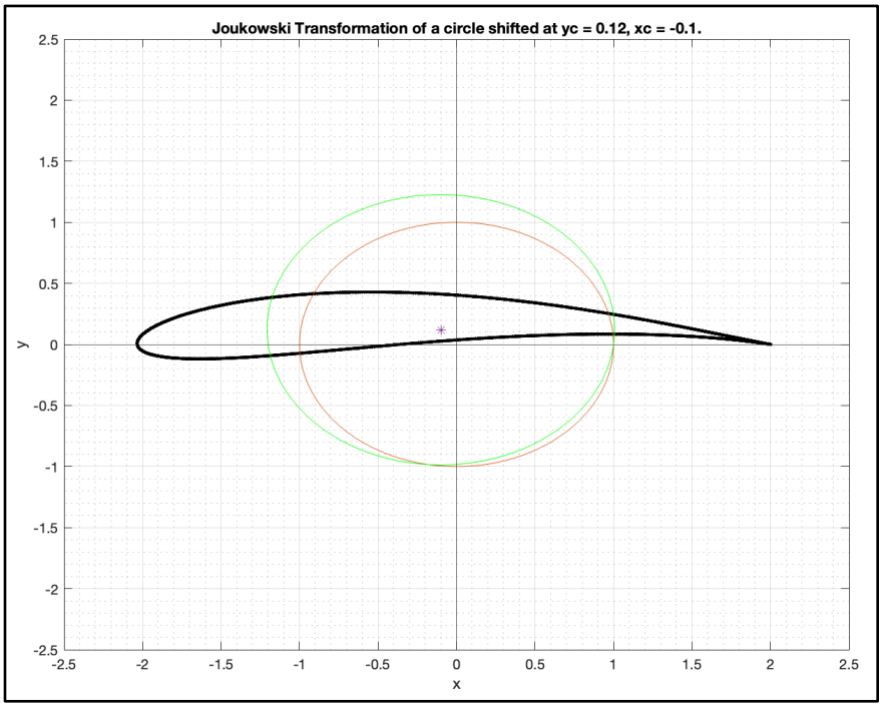

***Figure 2**: Joukowski Airfoil.*

Figure 2 illustrates the Joukowski Airfoil using a circle centered at X_c = -0.1 and Y_c = 0.12. Increasing the X_c variable increased the airfoil thickness and increasing the Y_c variable increased the airfoil camber. As seen in the figure, the airfoil as a very sharp trailing edge. The equations defining the upper and lower surfaces of the airfoil are a function of x and are as follows,

$$f_{lower\ surface}(x) = -0.0013x^9 + 0.0014x^8 + 0.0096x^7 - 0.0089x^6 - 0.0255x^5 + 0.0202x^4 + 0.0119x^3 - 0.0441x^2 + 0.085x + 0.0375$$

$$f_{upper\ surface}(x) = 0.0016x^9 - 0.0017x^8 - 0.012x^7 + 0.0108x^6 + 0.0319x^5 - 0.0242x^4 - 0.0199x^3 - 0.0608x^2 - 0.0834x + 0.4022$$

The thickness to chord ratio of this airfoil was calculated using the equations for upper surface and the lower surface as such:

$$maximum\ thickness\ \% = \frac{\max\left(\frac{Y_{upper} - Y_{lower}}{2}\right)}{chord} * 100\%$$

The maximum thickness for the Joukowski airfoil was calculated to be 4.6%. Using potential flow theory, the flow around the airfoil was computed with Joukowski transformation of the following stream function, where gamma is the circulation required to impose the kutta condition at the trailing edge.

$$\psi = U\left(r\sin(\theta - \alpha) - \frac{a^2}{r}\sin(\theta - \alpha)\right) + \frac{\Gamma}{2\pi}\ln(r)$$

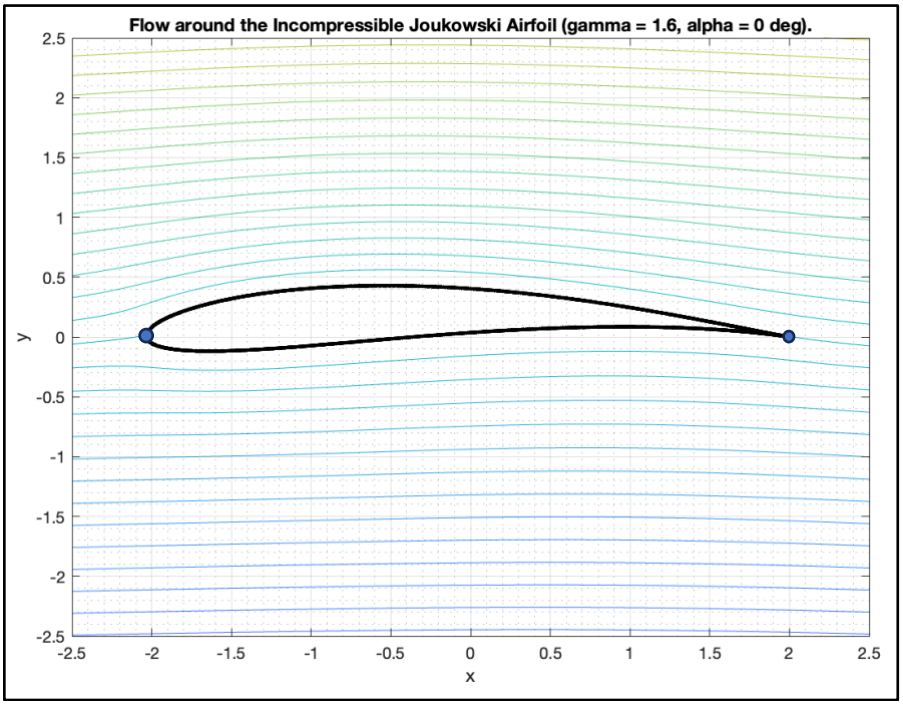

Figure 3: *Flow around incompressible Joukowski Airfoil.*

As seen in Figure 3, the dividing streamlines signifies the leading and trailing edges on the Joukowski airfoil as illustrated by blue dots. The flow around this airfoil was compute at an angle of attack of 0 degrees with a circulation (Γ) of 1.6, at which the kutta condition is imposed on the trailing edge cusp of the Joukowski airfoil. The pressure coefficient on the upper and lower surfaces of the airfoil are calculated as follows,

$$\beta = \tan^{-1}\frac{y_c}{1 - x_c}$$

$$Cp = 1 - \left\{ \frac{\|Z\|}{\left\|Z - \frac{1}{\bar{Z}}\right\|} \left[2\sin(\theta - \alpha) + \frac{\Gamma}{2\pi b} \right] \right\}^2$$

For upper surface: $-\beta \leq \theta \leq \pi + \beta$, and for lower surface: $\pi + \beta \leq \theta \leq 2\pi - \beta$. Thus, using the pressure distribution over the upper and lower surface, the delta Cp equation is integrated over the airfoil chord to compute incompressible Joukowski airfoil lift coefficient. The lift coefficient was calculated to be 0.6854, at a 0 angle of attack and with circulation of 1.6.

Karman-Trefftz Airfoil

As seen in the previous section, the Joukowski airfoil presented in Figure 2 has a very sharp trailing edge. Although the Joukowski airfoil makes sense mathematically, and its analysis is still valid, however, to manufacture an airfoil with an infinitesimally small thickness at the trailing edge is impossible. Thus, a Karman Trefftz transformation is used to add a thickness on the trailing edge of the Joukowski airfoil. This is achieved by using the following transformation:

$$\zeta = Z + \frac{k^2 - 1}{3Z}, 1 < k < 2$$

The constant 'k' is found to be somewhere between 1 and 2. As 'k' approaches 1, the Joukowski airfoil becomes a 'circular blob' and as 'k' approaches 2, the sharp trailing edge of the Joukowski airfoil changes to a round cusp. After testing the implication of different 'k' values on the airfoil thickness, a Karman-Trefftz airfoil was generated at k = 1.93 and is presented in Figure 4. The figure also illustrates a comparison between the Joukowski airfoil and the Karman-Trefftz airfoil. The Karman-Trefftz airfoil has a slightly smaller chord and a slightly higher thickness as a result of changing the 'k' parameter. The trailing edge also changes and features a small cusp for the Karman-Trefftz airfoil. A drawback of using a Karman-Trefftz transformation is that it can modify the positions of the leading and trailing edge stagnation points as seen in the figure. This shift in the trailing edge position affects the "circulation," influencing the generated lift and the angle of attack. Notice that at 'k' equals 1, the airfoil transforms to a circle centred at X_c = -0.1 and Y_c = 0.12 and at 'k' equals 2, the airfoil is similar to the Joukowski airfoil.

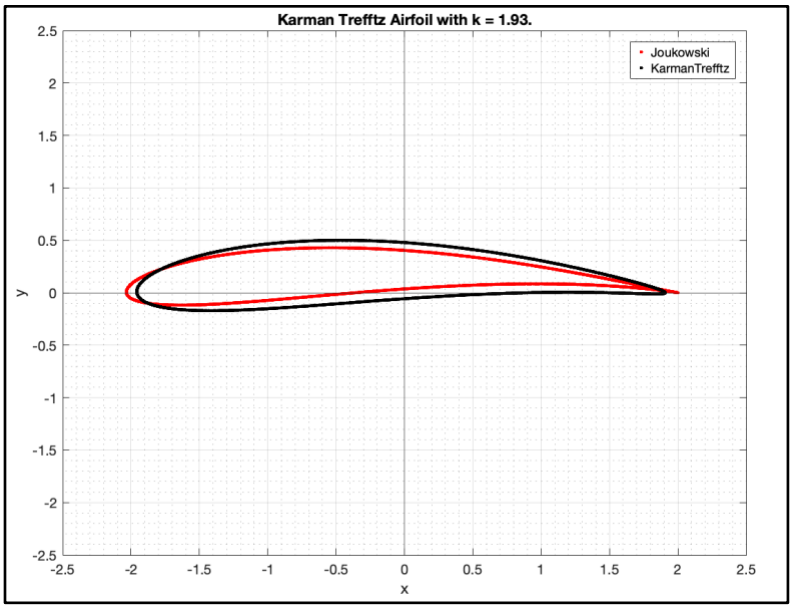

Figure 4: *Karman-Trefftz Airfoil with k = 1.93.*

Figure 5 illustrates the flow around the Karman-Trefftz airfoil. Since the thickness of the airfoil increases slightly, the circulation (Γ) also increases from 1.6 to 1.75 for the Karman-Trefftz airfoil design to impose kutta condition at the trailing edge. Although the angle of attack remains constant in this particular case. The stagnation points, and the leading and trailing edges of the airfoil are also defined by the dividing streamlines as seen through blue dots in Figure 5.

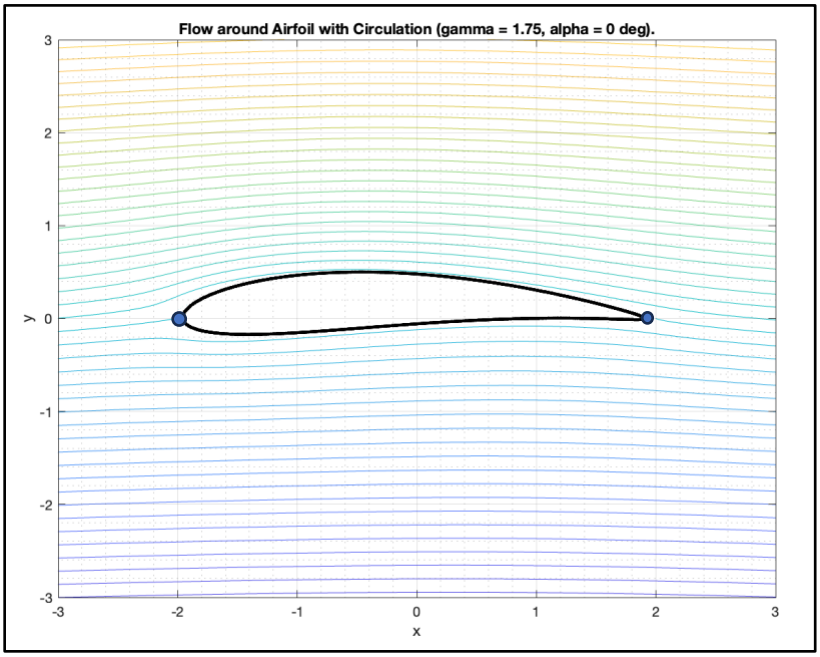

Figure 5: *Flow around incompressible Karman-Trefftz Airfoil.*

Using the definition of the leading and trailing edge points seen in Figure 5, the airfoil surface is divided in two halves, upper surface and a lower surface. The equations defining the upper and lower surfaces of the airfoil are a function of x and are as follows,

$$f_{upper\ surface}(x) = 0.0023x^9 - 0.0035x^8 - 0.0164x^7 + 0.0206x^6 + 0.0409x^5 - 0.0422x^4 - 0.0258x^3 - 0.0664x^2 - 0.0825x + 0.4765$$

$$f_{lower\ surface}(x) = 0.0016x^{12} - 6.8968 * 10^{-4}x^{11} - 0.0155x^{10} + 0.0063x^9 + 0.0577x^8 - 0.0211x^7 - 0.0983x^6 + 0.0296x^5 + 0.0781x^4 - 0.0304x^3 - 0.0417x^2 + 0.0936x - 0.0561$$

The maximum thickness of the Karman-Trefftz airfoil was calculated to be 6.7% and has increased as compared to the Joukowski airfoil which is also evident in Figure 4. Using the Karman-Trefftz transformation the pressure coefficient equation changes to become:

$$Cp = 1 - \left\{ \frac{\|Z\|}{\left\| Z - \frac{k^2 - 1}{3Z} \right\|} \left[2\sin(\theta - \alpha) + \frac{\Gamma}{2\pi b} \right] \right\}^2$$

For upper surface: $-\beta \leq \theta \leq \pi + \beta$, and for lower surface: $\pi + \beta \leq \theta \leq 2\pi - \beta$. The pressure coefficients are computed on the upper and lower surfaces and are presented in Figure 6.

As seen, the upper surface has a negative pressure distribution as the flow speeds increase over the top surface, and the lower surface has a positive pressure distribution.

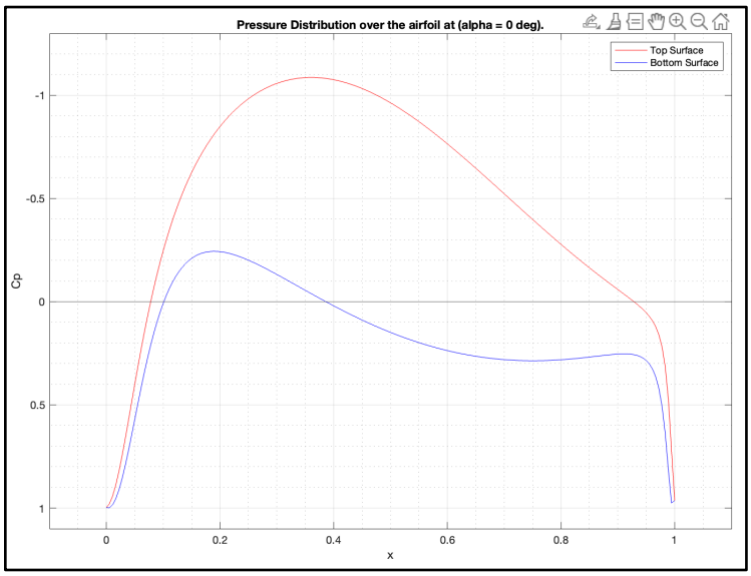

Figure 6: *Pressure Coefficient over the Karman-Trefftz Airfoil.*

The area under the graph for the pressure coefficient presented in Figure 6, is calculated by integrating the upper and lower pressure coefficient curves. This area signifies the total lift coefficient calculated for the Karman-Trefftz airfoil. The lift coefficient calculated for the Karman-Trefftz was 0.6839 as compared to the lift coefficient produced by a Joukowski airfoil of 0.6854, both at 0 angle of attack.

Thin Airfoil Theory

Now that an acceptable airfoil is designed according to my objectives presented in the previous sections. I wanted to check if the above Karman-Trefftz airfoil can be modelled as a thin airfoil. For this process the equations developed earlier for the upper and lower surface of the airfoil were used to generate a chamber line as seen in Figure 7.

$$Camber\ Line\ (y_c) = \frac{f_{upper\ surface}(x) + f_{lower\ surface}(x)}{2}$$

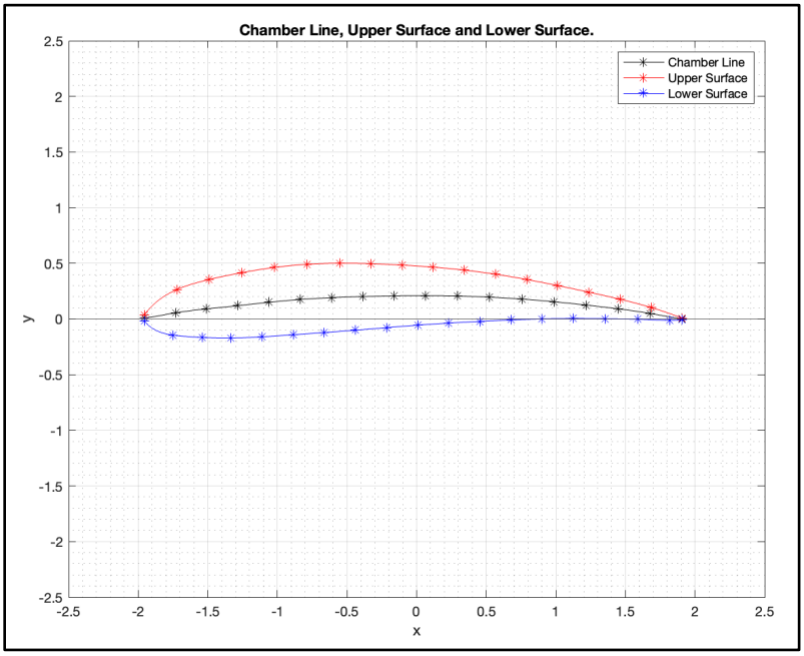

Figure 7: *Karman-Trefftz Airfoil with Camber Line.*

This method models the airfoil as a camber line. The Thin Airfoil Theory simplifies lift generation by assuming that it results from an idealized camber line created by an infinite series of vortices of varying strengths. In this approach, the airfoil's thickness is disregarded as well. The Thin Airfoil Theory also assumes that different pressure distributions above and below the theoretical camber line generate lift, which may not accurately reflect the true pressure distributions on the actual airfoil surfaces. A limitation of this approach is that Thin Airfoil Theory is strictly applicable to airfoils that are infinitely thin and operate at zero angle of attack. While

small angles of attack may still yield reasonable approximations, the accuracy depends on the airfoil's specific characteristics, including thickness, camber magnitude, and distribution.

The lift coefficient is calculated using a vortex approximation method. A distribution of point vortex is placed along the camber line with varying circulation 'k' values depending on the flow direction that follows the camber line. The circulation k is then given by:

$$k = 2U_\infty \left[(\alpha - A_0) \frac{(1 + \cos\theta)}{\sin\theta} + \sum_{n=1}^{\infty} A_n \sin N\theta \right]$$

However, using only the first term (until A_1) from the above summation (because terms after which are smaller than 10^{-5}), to approximate the lift coefficient:

$$Cl = \int_0^\pi k * \sin\theta \, d\theta = 2\pi(\alpha - A_0) + \pi A_1$$

$$\text{Where, } A_0 = \frac{1}{\pi}\int_0^\pi \frac{dy_c}{dx} d\theta \text{ and } A_1 = \frac{2}{\pi}\int_0^\pi \frac{dy_c}{dx} \cos\theta \, d\theta$$

The thin airfoil lift coefficient for the Karman-Trefftz airfoil was calculated to be 0.6863. The term $\alpha - A_0 = 0$, represents the ideal angle of attack for the camber line. The ideal angle of attack was calculated to be -3.2558 degrees. The thin airfoil lift coefficient was calculated at an angle of attack of 0 degrees. Since, the designed Karman-Trefftz airfoil has a Cl of 0.6839 at a 0 angle of attack, it can therefore be considered as a thin airfoil. When operating at the optimum angle of attack, the Karman-Trefftz airfoil generates a lift coefficient of 0.5 with a circulation (Γ) of 1.35.

Inverse Design

This section explores in calculating the camber line of the Karman-Trefftz airfoil using an inverse design method. For This method, the pressure distribution plot in Figure 6 is used to compute the camber line as follows:

$$A_o = -\alpha$$

$$A_1 = \frac{1}{2\pi}\int_0^\pi \Delta C_p \sin\theta \, d\theta$$

$$y_c = k - \alpha x + \int A_1 \left(1 - \frac{2x}{c}\right) dx$$

For this study, only two terms (up to A_1) are used. As seen in the previous section, 'k' is a constant that adds up the circulation for each point vortex along the camber line. Therefore, the camber line calculated this inverse design method is presented in Figure 8.

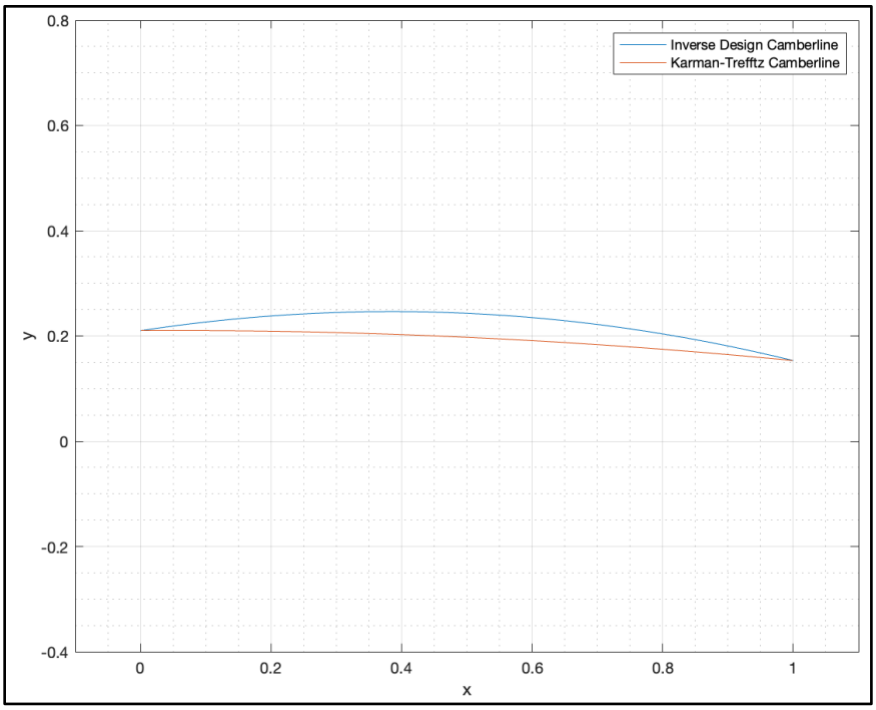

Figure 8: *Inversely Designed Camber line.*

As see, the camber line using the inverse design method estimates a higher camber as compared to the actual Karman-Trefftz airfoil camber line. This difference could have risen from the fact that only two terms (A_o and A_1) were used to approximate the curve equation Y_c. This exercise signifies that the inverse design method can be used as a good approximation tool to calculate the camber line of an airfoil given its pressure distribution.

Compressible Design

Now that the lift coefficient is analyzed using the thin airfoil theory, this section analyzes the compressible effects on the designed incompressible Karman-Trefftz airfoil. To do this, a critical pressure or the minimum pressure is calculated on the upper surface of the airfoil by using the incompressible Cp equation presented in above sections. The minimum pressure coefficient was calculated to be -1.0859 as seen in Figure 8 represented by a dashed line. Using this, a design Mach number of the airfoil is calculated as follows:

$$Cp_{min} = Cp_{critical} = \frac{2}{\gamma * M_{design}^2}\left\{\left[\frac{1+\frac{\gamma-1}{2}M_{design}^2}{1+\frac{\gamma-1}{2}}\right]^{\frac{\gamma}{\gamma-1}} - 1\right\}$$

$$Cp_{comp} = \frac{Cp_{incomp}}{\sqrt{1-M_{design}^2}}, Cl_{comp} = \frac{Cl_{incomp}}{\sqrt{1-M_{design}^2}}$$

The design compressible Mach number for the Karman-Trefftz airfoil was calculated to be 0.6356. Using the above Prandtl-Glauert relationship, the compressible pressure coefficient over the airfoil was calculated and is presented as a solid blue line in Figure 8. The compressible Cl was calculated to be 0.8855.

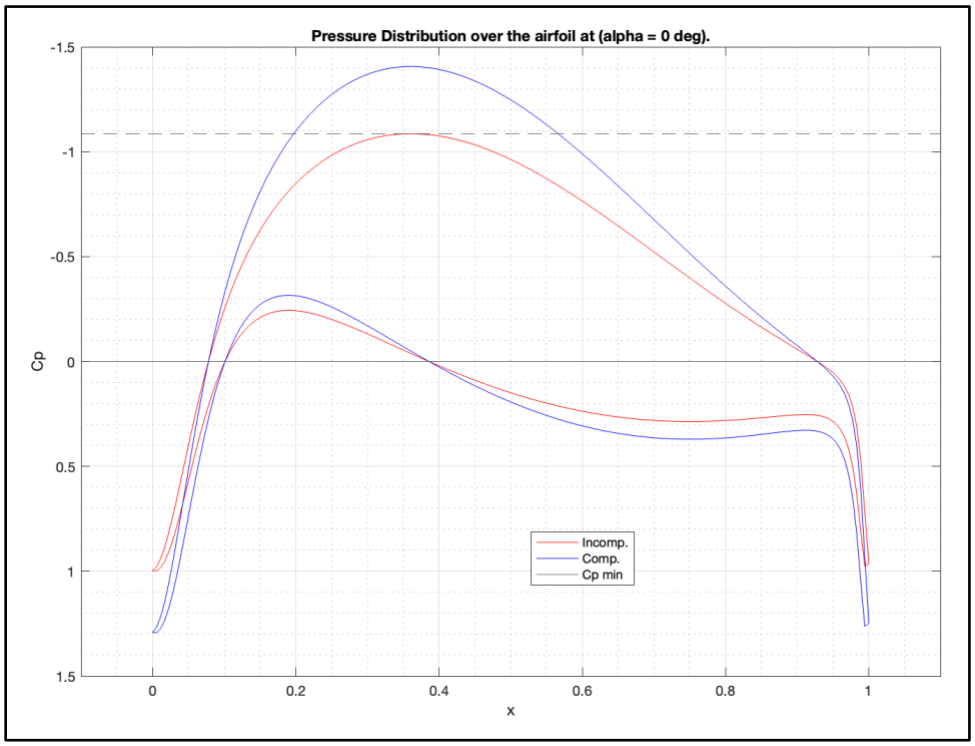

Figure 9: *Incompressible and Compressible Pressure coefficient Distributions over the airfoil.*

Since the Cp compressible graph for the compressible flow goes over the critical pressure line, a normal shock exists on the upper surface of the airfoil. The x-location of the shock over the upper surface is determined by the minimum pressure coefficient for the compressible flow. The minimum pressure coefficient for the compressible Cp is calculated to be -1.4061 at a x-location of 0.36 (or 36% chord from leading edge). Since the flow is assumed isentropic before the normal shock wave, the following isentropic relationships are used:

$$\frac{P_s}{P_\infty} = \frac{Cp_s * \gamma * M_{design}^2}{2} + 1 = 0.6027$$

$$\frac{P_o}{P_\infty} = \left(1 + \frac{\gamma - 1}{2} M_{design}^2\right)^{\frac{\gamma}{\gamma - 1}} = 1.3122$$

$$\frac{P_s}{P_o} = \frac{P_s}{P_\infty} * \frac{P_\infty}{P_o} = 0.4593$$

$$M_s = \sqrt{\left[\left(\frac{P_o}{P_s}\right)^{\frac{\gamma-1}{\gamma}} - 1\right] * \frac{2}{\gamma - 1}}$$

At the computed x-location presented above, on the upper surface, the Mach number before the normal shock is calculated to be 1.1156 using the above isentropic relationships.

$$M_2 = \sqrt{\frac{M_s^2 + \frac{2}{\gamma - 1}}{\frac{2\gamma}{\gamma - 1} M_s^2 - 1}}$$

$$\frac{P_2}{P_s} = \frac{2\gamma M_s^2}{\gamma + 1} - \frac{\gamma - 1}{\gamma + 1}$$

The above normal shock relationship is used to calculate the Mach number after the normal shockwave. The Mach number is calculated to be 0.8998. The ratio between the static pressures across the shock is calculated to be 1.2854. This makes sense because, across the shock the velocity decreases, along with total pressure however the static pressure increases.

$$Cp_{sub} = \frac{2}{\gamma * M_{design}^2} \left(\frac{P_s}{P_\infty} * \frac{P_2}{P_s} - 1 \right)$$

The pressure coefficient at the subsonic speed after the normal shock is calculated to be -0.7973. This results in an overall lift loss due to the shock on the upper surface. The pressure loss on the upper surface is calculated by subtracting the shaded region from the compressible Cp upper equation. The area bounded by the solid vertical and horizontal black lines, the red solid line for the upper surfaces and the blue solid line for the lower surface, represents the delta Cp as a result of the normal shock. This is illustrated in Figure10. The total lift generated, and the subsequent lift loss are calculated by integrating the area enclosed by Cp upper, lower and the Cp lost due to normal shock.

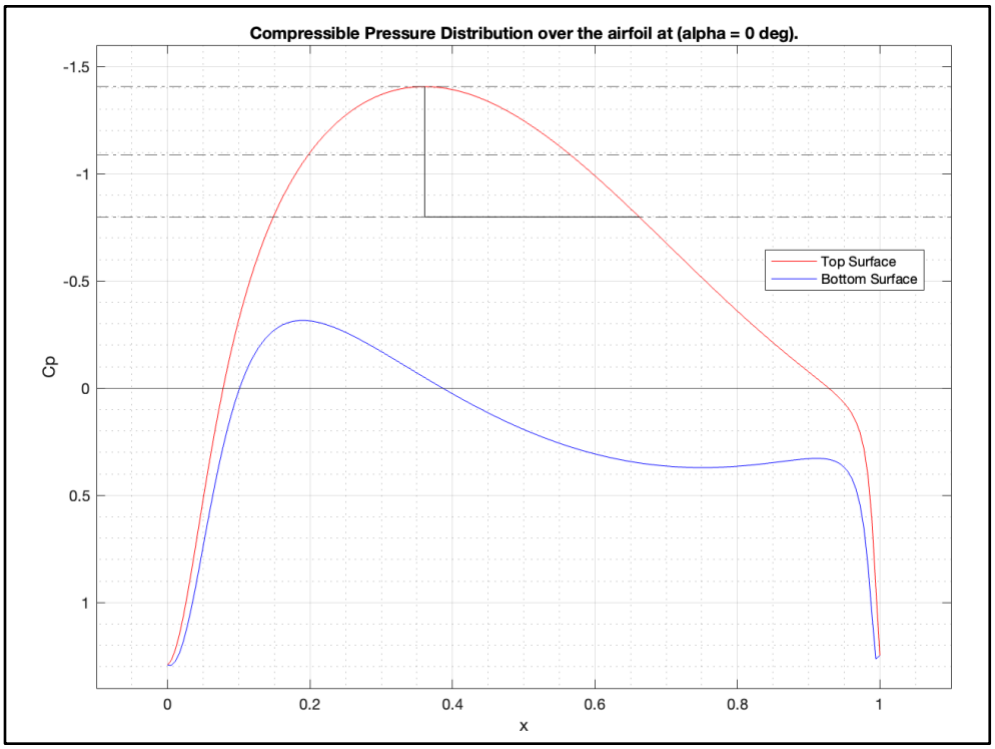

Figure 10: *Compressible Pressure Distribution over the airfoil with Normal Shock losses.*

The total lift coefficient losses due to the normal shock is calculated to be 0.1883. Thus, under the compressible flow analysis, the Karman-Trefftz airfoil produces a lift coefficient of 0.6972 at a Mach number of 0.6356. The total lift losses account for approximately 21% of total lift if no shock were present. This is a major loss of lift and thus a redesign of the bottom surface is required to add back the lift losses caused due to the normal shock. The redesign of the bottom surface is done by adding the area of pressure loss seen in Figure 9 to the bottom surface and then recreating the bottom surface using Joukowski transformation and Karman-Trefftz transformations. As a rough estimate, the new airfoil should atleast produce a Cl of 1.0739 in compressible conditions and a Cl of 0.8293 under incompressible conditions.

Airfoil Redesign

As seen in Figure 11 below, the red solid curve represents the pressure distribution on the upper surface, and the area bounded by this and the dashed red curve represents the pressure lost and thus the lift loss due to the normal shock. This area is added to the bottom surface, therefore the new pressure distribution required to negate the loss of lift due to the normal shock is represented by the solid blue curve, whereas the dashed black curve represents the old pressure distribution similar to Figure10. Integrating the area under the graph, with the added life losses, the redesigned airfoil must generate a Cl of 1.0739 in compressible conditions and a Cl of 0.8293 under incompressible conditions.

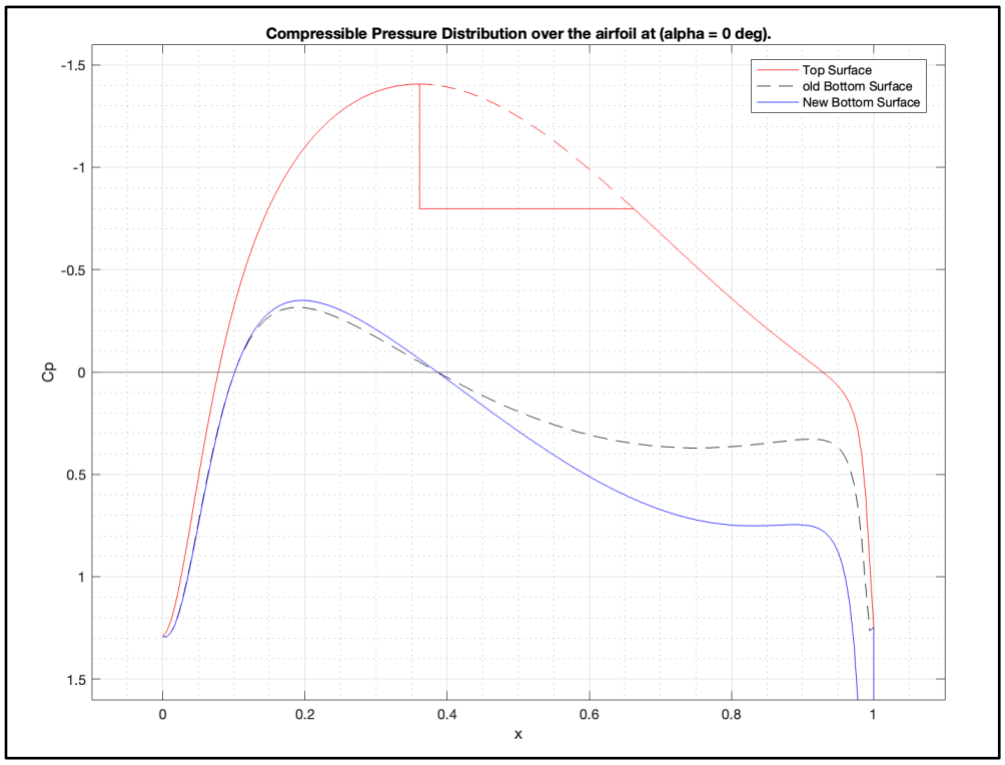

Figure 11: *Adding the Lost Cp from Upper Surface onto the Lower Surface.*

The old Cp lower equation is modified as such, where A and B are real constants that generate a new Cp lower equation. This specific term is used so that for B values higher than 1, only the latter half of the curve changes while the leading-edge portion remains the un-altered. Additionally, as 'A' is decreased, the slope for Cp lower curve increases negatively such that the blue curve is pushed down after x = 0.4 and pushed up before x = 0.4.

$$New\ Cp_{lower} = Cp_{lower}(x, x_c, y_c, \Gamma, \alpha, \mathrm{k}) * (1 - A * x^B)$$

The new cp lower curve in Figure 11 is calculated using the values for A = -1.75 and B = 0.8. At these set coefficients, the compressible lift coefficient is calculated to be 1.0739 without accounting for the lift losses.

For the redesigned lower surface pressure coefficient at compressible speeds, the pressure coefficients on the upper and lower surfaces are converted back to incompressible speeds using the Prandtl-Glauert relations seen previously.

The goal of this final task is to design a Joukowski airfoil with a new lower surface that produces the same pressure coefficient curve as compared to the above redesigned curve in Figure 11. After this the new airfoil is sliced and only the bottom surface is used and merged with the top surface from the original incompressible Joukowski airfoil. This way, the pressure coefficient for the final airfoil will have a favorable pressure coefficient curve that account for the lift losses due to a normal shock on the upper surface.

Redesigning a new Joukowski airfoil meant changing the $X_c, Y_c, \alpha, and\ \Gamma$ variables to generate the desired lower cp curve. For this analysis, all four variables were changed and a following Joukowski airfoil is created:

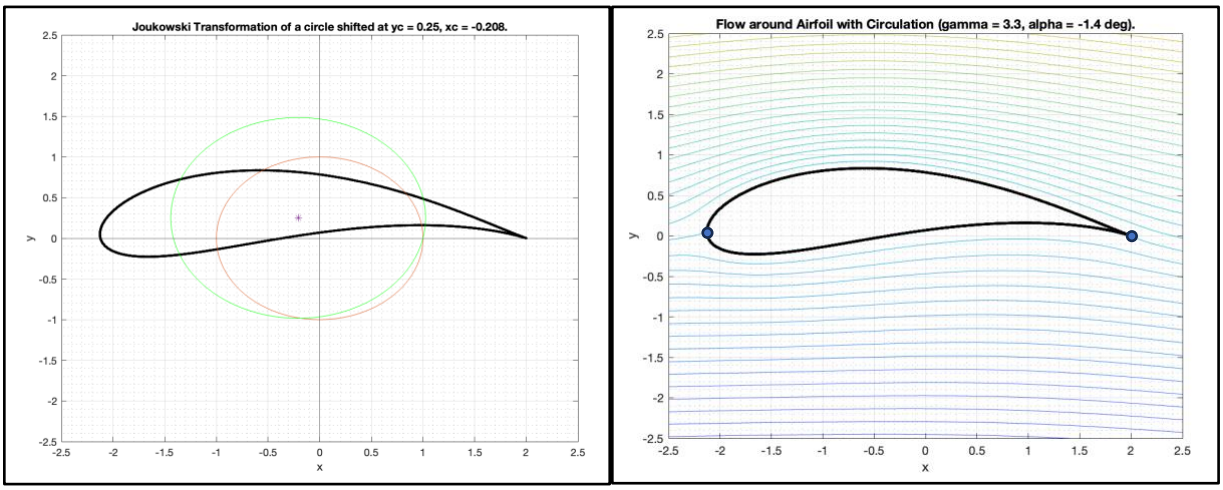

Figure 12: *New Joukowski Airfoil and flow around it.*

Figure 12 illustrates a new airfoil with $X_c, = -0.208, Y_c = 0.25, and\ \alpha = -1.4$ and the flow around the airfoil at the given angle of attack. As seen the with circulation (Γ) = 3.3, enforces a kutta condition at the trailing edge of the airfoil.

As seen in Figure 13, the blue dotted curve illustrates the cp curve corresponding to the new bottom surface generated from the above Joukowski airfoil parameters. In the same figure, the black dotted curves represent the ideal incompressible cp required to negate the cl losses at compressible speeds similar to Cp presented in Figure 11.

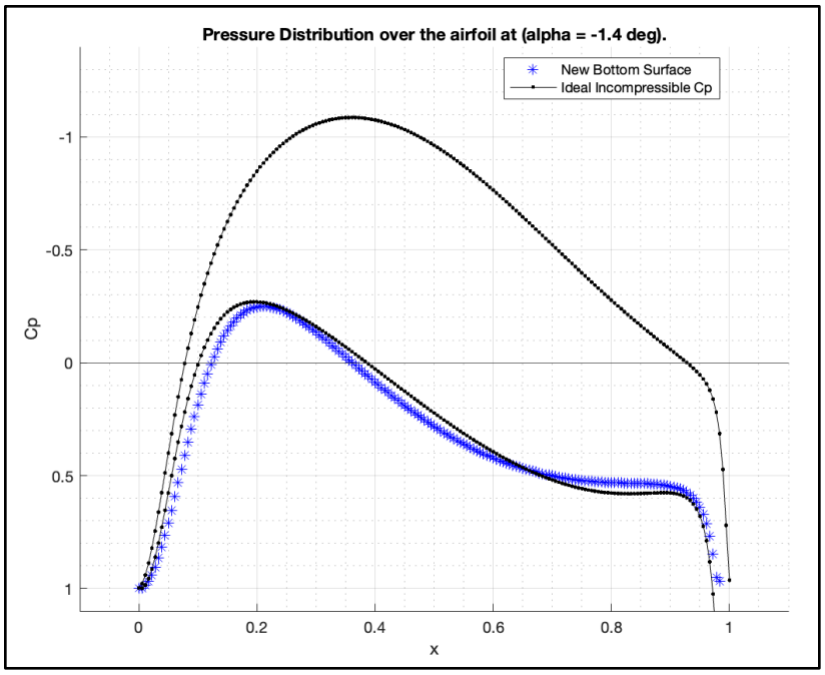

Figure 13: *Pressure Distribution over the new airfoil.*

Now that we have the required cp lower distribution and the cp lower curve corresponding to this, the top surface from the original airfoil is merged with the bottom surface of the new airfoil as illustrated in Figure 14 (right most plot). The left most plot compares the original and the new airfoils. As seen, since the new airfoil as a higher X_c *and* Y_c constants, the new airfoil is much thicker and has a greater camber as well.

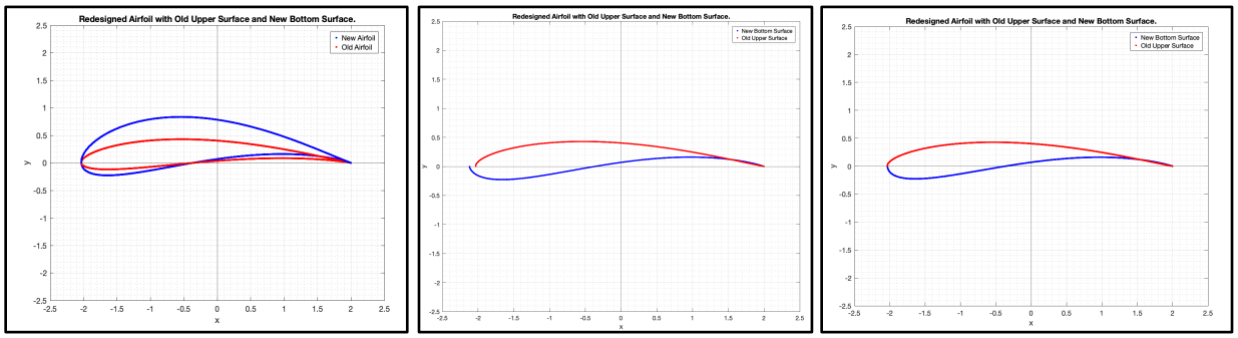

Figure 14: *Redesigned Airfoil by merging the original upper surface and a new lower surface Using Joukowski Transformation.*

However, when merging the two surfaces, it is seen (from the middle plot) that the leading edges of the upper and lower surfaces don't align at the same x-locations. This is because, for this analysis, X_c is also changed when designing the new Joukowski airfoil. To fix this, either X_c has to remain unchanged for the redesign (compared to the original Joukowski airfoil) or a correction parameter can be used to normalize the x-values of the new lower surface. For this study a correction factor is used to normalize the x-values and then reparametrize the lower surface based on the x-values of the upper surface.

$$x_{lower} = \frac{x_{lower}}{x_{lower}} * x_{upper}$$

However, using the above correction parameter, the lower surface curve changes slightly at the leading edge. The correction parameter has a squeezing effect on the curve. Therefore, for the redesigned airfoil, the updated cp coefficient curve is calculated and presented as follows in Figure 15. Integrating the area under the graph, the incompressible cl is calculated to be 0.8304 and the compressible cl is calculated to be 1.075 at a design Mach number of 0.6353.

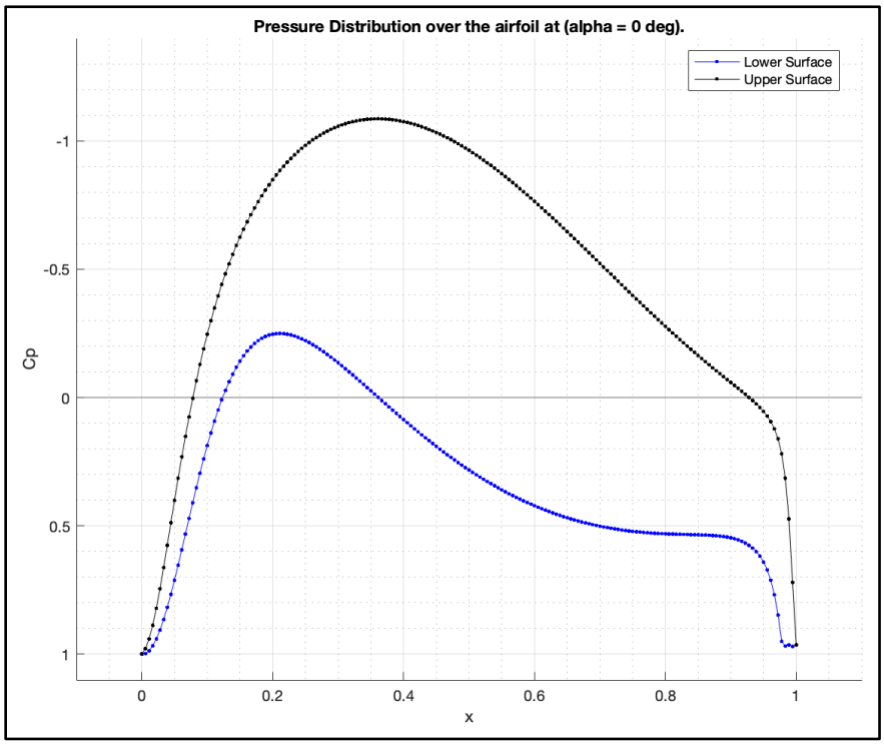

Figure 15: *Incompressible Pressure Distribution over the Redesigned Airfoil.*

However, as seen in Figure 14, in the right most plot, the trailing edges for the upper and lower surfaces intersect and cross over near the trailing edge. This is a common occurrence when merging two Joukowski airfoils for the redesign. Since, this airfoil design is good enough for the analysis process, it is not good enough for its manufacturing. Thus, a thickness is required at the trailing edge. For this task, two Karman-Trefftz airfoils are merged. The exercise remains the same as before, but in this case, the upper surface of the original Karman-Trefftz is used to merge with a lower surface from a new Karman-Trefftz airfoil that matches with the ideal cp lower curve seen in Figure 13.

Figure 16 illustrates the new Karma-Trefftz airfoil using a ‘k’ factor of 1.93 (same as the one for the original Karman-Trefftz airfoil). The left figure compares the original Karman-Trefftz airfoil and the new Karman-Trefftz airfoils. As seen, the trailing edge is no more a sharp edge but has a smooth cusp. The right figure illustrates the merged redesigned airfoil.

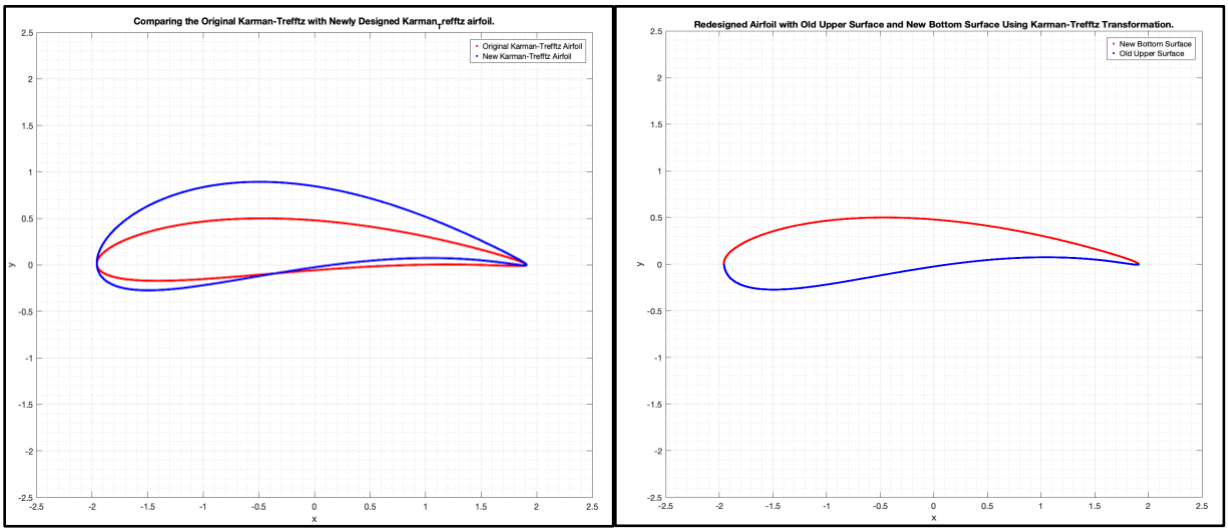

Figure 16: *Redesigned Airfoil by merging the original upper surface and a new lower surface Using Karman-Trefftz Transformation.*

The redesigned Karman-Trefftz airfoil has an incompressible Cl of 0.8373 and a compressible Cl of 1.0842. This is higher than the design approximations discussed at the start of this section. The Cp distribution for the above redesigned Karman-Trefftz airfoil is presented in Figure 17.

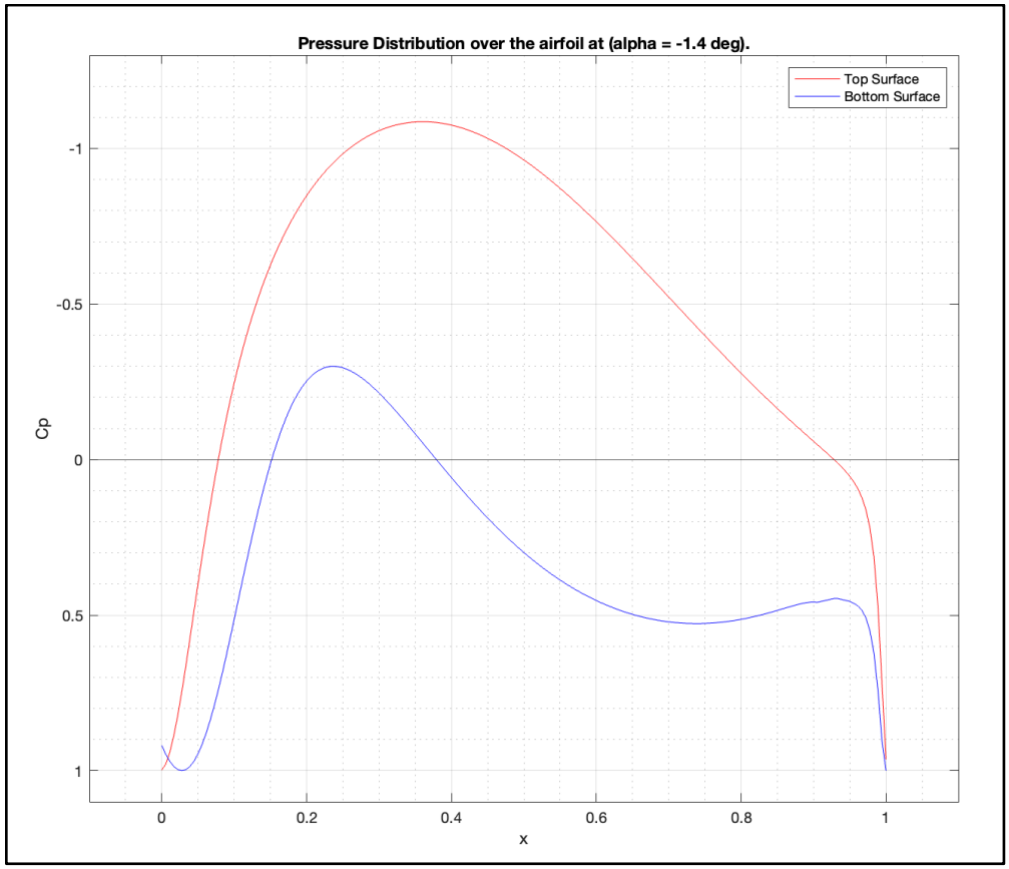

Figure 17: *Pressure Distribution over the Redesigned Karman-Trefftz Airfoil.*

Using the developed equations for the upper and lower surface of the redesigned Karman-Trefftz airfoil (presented below), the camber line was calculated as well using the equation presented in previous section.

$$f_{upper\ surface}(x) = 0.0023x^9 - 0.0035x^8 - 0.0164x^7 + 0.0206x^6 + 0.0409x^5 - 0.0422x^4 - 0.0258x^3 - 0.0664x^2 - 0.0825x + 0.4765$$

$$f_{lower\ surface}(x) = -0.0033x^9 + 0.0046x^8 + 0.0231x^7 - 0.0264x\text{^}6 - 0.0571x^5 + 0.0548x^4 + 0.0254x^3 - 0.0819x^2 + 0.1599x - 0.0229$$

The camber line is presented in Figure 18 below. The camber line is used to estimate the thin airfoil lift coefficient.

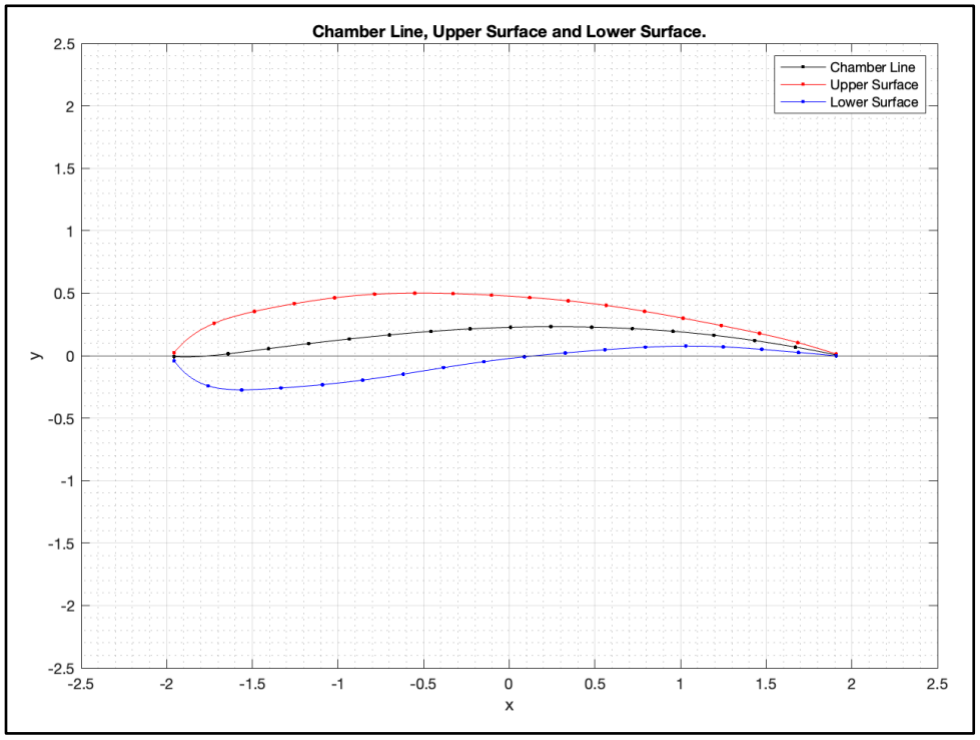

***Figure 18**: Redesigned Karman-Trefftz Airfoil with Camber line.*

Using the similar methodology presented earlier, the thin airfoil Cl is calculated to be 0.8348 at a 0 angle of attack. With the incompressible Cl of 0.8373 calculated for the redesigned Karman-Trefftz airfoil, it can be concluded that this is a thin airfoil. The ideal angle of attack for the redesigned airfoil is calculated to be -2.1674 degrees. At this angle of attack, the cl is calculated to be 0.2462.

Discussion and Results

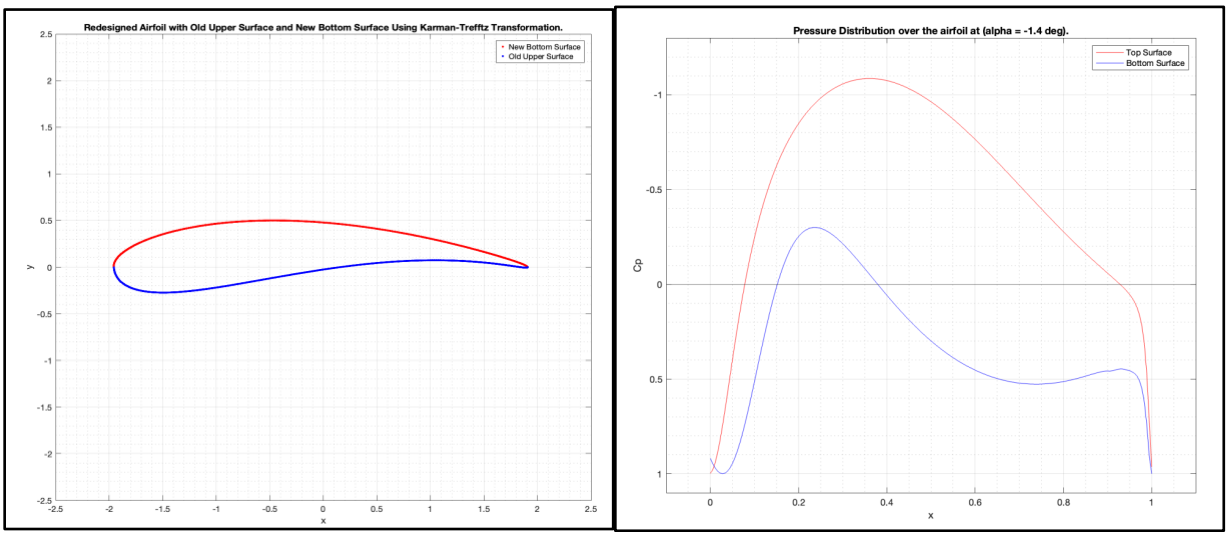

Figure 19: *Final Airfoil.*

Based on the final redesigned Airfoil, as seen in figure 19, it features a Karman-Trefftz airfoil. The airfoil has an incompressible Cl of 0.8373 and a compressible Cl of 1.0842 at the design Mach number of 0.6353 and angle of attack 0. The airfoil can also be analyzed as a thin airfoil, and the thin airfoil Cl was calculated to be 0.8348 at 0 angle of attack. The ideal angle of attack calculated for this airfoil is -2.2 degrees. The redesigned airfoil has a thickness to chord ratio of 6.6%.

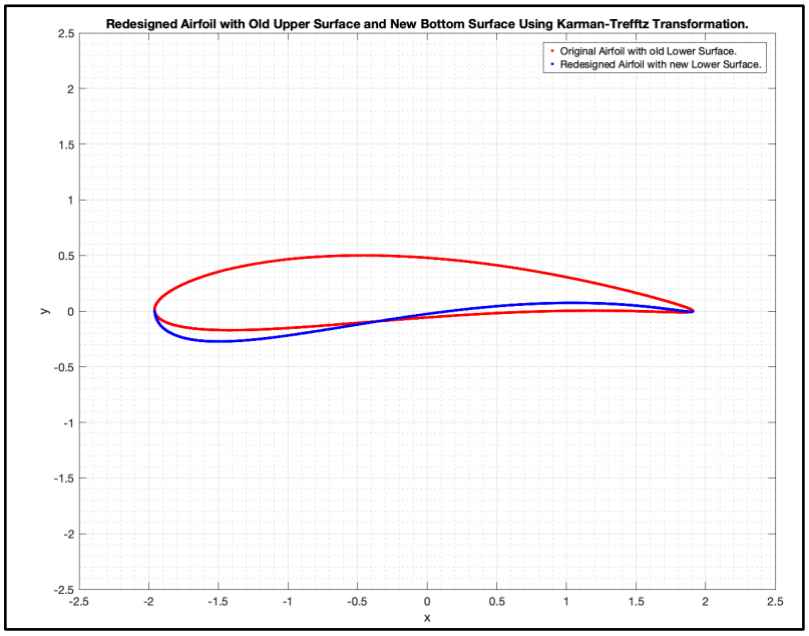

Figure 20*: Comparing the Original and Redesigned Airfoils.*

The redesign process altered the positions of the leading and trailing edges slightly due to adjustments in the camber and thickness distributions. This was observed particularly when merging upper and lower surfaces of new and original airfoils. The maximum thickness of the airfoil decreased slightly from 6.7% to 6.6%. However, the thickness distribution over the chord line has changed significantly. This change aimed to compensate for lift losses caused by the shock wave. The ideal angle of attack for the redesigned Karman-Trefftz airfoil increased slightly compared to the original airfoil from -3.2558 to -2.1674 degrees. The camber line of the redesigned airfoil shifted to accommodate the new lower surface. The camber line for the redesigned airfoil illustrates a higher camber.

Redesigning an airfoil reveals that changes in one parameter, such as the lower surface pressure distribution, inherently affect others, including camber line, thickness, and leading/trailing edge positions. The critical elements to control are:

- Leading and trailing edge locations, as they influence stagnation points and is important while imposing the kutta condition through changing the circulation.
- Camber line geometry, as it directly determines lift and angle of attack through thin airfoil theory.
- Pressure distributions (Cp upper and Cp lower) to optimize lift and mitigate losses due to shocks or compressibility effects.

References

[1] ‘Transonic Airfoils for Propellers ’. Accessed: Dec. 04, 2024. [Online]. Available: https://www.supercoolprops.com/articles/transonic.php